Accepted Manuscript

Neuroprotective effects of the cannabinoid agonist HU210 on retinal degeneration

Pedro Lax, Gema Esquiva, Cesare Altavilla, Nicolás Cuenca

PII: S0014-4835(14)00034-7

DOI: 10.1016/j.exer.2014.01.019

Reference: YEXER 6362

To appear in: *Experimental Eye Research*

Received Date: 6 September 2013

Revised Date: 20 January 2014

Accepted Date: 24 January 2014

Please cite this article as: Lax, P., Esquiva, G., Altavilla, C., Cuenca, N., Neuroprotective effects of the cannabinoid agonist HU210 on retinal degeneration, *Experimental Eye Research* (2014), doi: 10.1016/j.exer.2014.01.019.

Title: Neuroprotective effects of the cannabinoid agonist HU210 on retinal degeneration

Author names and affiliations: Pedro Lax [a,*], Gema Esquiva [a,*], Cesare Altavilla [a] and Nicolás Cuenca [a,b]

[a]Department of Physiology, Genetics and Microbiology, University of Alicante, Alicante, Spain.

[b]Institute Ramón Margalef, University of Alicante, Alicante, Spain.

*These authors contributed equally to the work presented here and should therefore be regarded as equivalent authors.

Corresponding author: Nicolás Cuenca, Department of Physiology, Genetics and Microbiology, University of Alicante, San Vicente University Campus, E-03080 Alicante, Spain; Phone: +34965909916, Fax: +34965903943, E-mail: cuenca@ua.es

ABSTRACT

Cannabinoids have been demonstrated to exert neuroprotective effects on different types of neuronal insults. Here we have addressed the therapeutic potential of the synthetic cannabinoid HU210 on photoreceptor degeneration, synaptic connectivity and functional activity of the retina in the transgenic P23H rat, an animal model for autosomal dominant retinitis pigmentosa (RP). In P23H rats administered with HU210 (100 μg/kg, i.p.) from P24 to P90, ERG recordings showed an amelioration of vision loss, as compared to vehicle-administered animals. Under scotopic conditions, the maximum a-wave amplitudes recorded at P60 and P90 were higher in HU210-treated animals, as compared to the values obtained in untreated animals. The scotopic b-waves were significantly higher in treated animals than in untreated rats at P30, P60 and P90. This attenuation of visual deterioration correlated with a delay in photoreceptor degeneration and the preservation of retinal cytoarchitecture. HU210-treated animals had 40% more photoreceptors than untreated animals. Presynaptic and postsynaptic elements, as well as the synaptic contacts between photoreceptors and bipolar or horizontal cells, were also preserved in HU210-treated P23H rats. These results indicate that HU210 preserves cone and rod structure and function, together with their contacts with postsynaptic neurons, in P23H rats. These data suggest that cannabinoids are potentially useful to delay retinal degeneration in RP patients.

Key words: Neurodegeneration, retinitis pigmentosa, P23H, apoptosis, electroretinography, immunohistochemistry, confocal microscopy

Abbreviations: CB1 and CB2, Cannabinoid receptor type 1 and 2; ERG, electroretinogram; GCL, ganglion cell layer; INL, inner nuclear layer; IPL, inner plexiform layer; IS, inner segment; ONF, optic nerve fibers; ONL, outer nuclear layer; OPL, outer plexiform layer; OS, outer segment; PB, phosphate buffer; PKC-α, α isoform of protein kinase C; *RHO,* rhodopsin-encoding gene; RP, retinitis pigmentosa; ROS, reactive oxygen species; SYP, synaptophysin; THC, Δ^9-tetrahydrocannabinol

1. Introduction

Retinitis pigmentosa (RP) is a family of inherited neurodegenerative retinal disorders with an incidence in humans of approximately 1/4000 (Hartong et al., 2006). The disease is characterized by a progressive peripheral vision loss and night vision difficulties, subsequently leading to central vision impairment. More than 100 different mutations in the rhodopsin-encoding gene (*RHO*) are associated with RP, together accounting for 30-40% of autosomal dominant cases. The P23H mutation in this gene is the most prevalent cause of RP (Dryja et al., 1990), which alone accounts for approximately 12% of autosomal dominant RP cases in the United States (Dryja et al., 2000). The majority of RP-causing mutations in the *RHO* gene, including P23H, cause misfolding and retention of rhodopsin in the endoplasmic reticulum of transfected cultured cells (Kaushal and Khorana, 1994). These studies also suggest that the mechanism of RP involves a cellular stress response (Illing et al., 2002), the final common pathway being programmed photoreceptor cell death, or apoptosis (Reme et al., 1998). P23H transgenic albino rats suffer from a progressive retinal degeneration, which is consistent with the clinical findings in P23H patients (Berson et al., 1991; Cuenca et al., 2004; Machida et al., 2000; Pinilla et al., 2005). The loss of photoreceptors is accompanied by degenerative changes in the inner retina (Cuenca et al., 2004), and a substantial degeneration of retinal ganglion cells (Garcia-Ayuso et al., 2010; Kolomiets et al., 2010).

Several strategies are being investigated to slow or cure this group of diseases. Gene therapy, encapsulated cells releasing neurotrophic factors and stem cell transplantation are promising future approaches to RP treatment (Fernandez-Sanchez et al., 2012b; Musarella and Macdonald, 2011; Stieger,

2010). Molecules that promote survival, such as brain-derived neurotrophic factor, ciliary neurotrophic factor, fibroblast growth factor, glial-derived neurotrophic factor, pigment epithelium-derived factor, and proinsulin (Fernandez-Sanchez et al., 2012b), are moderately successful in preventing the progression of the disease when used in animal models (Cayouette et al., 1998; Cayouette et al., 1999; Chong et al., 1999; Green et al., 2001; McGee Sanftner et al., 2001; Okoye et al., 2003). Antioxidants have also been shown to be effective in preventing retinal degeneration in animal models of RP, probably by reducing oxidative damage (Ahuja et al., 2005; Berson et al., 1993; Fernandez-Sanchez et al., 2012a; Komeima et al., 2006; Lax et al., 2011). Finally, attenuation of apoptosis represents a good therapeutic target in RP, especially considering the vast heterogeneity of the disease (Doonan and Cotter, 2004; Fernandez-Sanchez et al., 2011; Liang et al., 2001). In the meantime, it would be thus interesting to address other potential treatments making it possible, if not to cure, at least to delay RP progression in the short term.

Cannabinoids have been reported to attenuate brain damage caused by different types of insults (Fernandez-Ruiz et al., 2010; Pertwee, 2012; van der Stelt and Di Marzo, 2005; Zogopoulos et al., 2013). Previous studies have shown neuroprotective effects of cannabinoids in the retina (Yazulla, 2008). Thus, it is known that CB1 agonists protect ganglion cells from glutamate-mediated excitotoxicity (El-Remessy et al., 2003; Opere et al., 2006) and ischemia caused by increased intraocular pressure (Crandall et al., 2007; Nucci et al., 2007; Pinar-Sueiro et al., 2013). HU210 is a synthetic analogue of Δ^9-tetrahydrocannabinol (THC), the primary psychoactive constituent in marihuana (Mechoulam et al., 1988). The aim of this study was to evaluate, by means of

functional (ERG) and morphological (histological labeling) techniques, the effectiveness of HU210 as a neuroprotective agent on homozygous P23H line 3 rats, characterized by a relatively slow retinal degeneration. Since one of the first signs of degeneration in these animals was found in the outer plexiform layer (OPL) (Cuenca et al., 2004; Pinilla et al., 2005), we also evaluated its capacity to prevent the loss of synaptic contacts at this retinal location. A positive assessment of the action of cannabinoids in this animal model could lead to its possible preventive use in patients affected with RP.

2. Materials and methods

2.1. Animals and HU210 administration

Homozygous P23H line 3 rats, obtained from M. LaVail (UCSF School of Medicine; http://www.ucsfeye.net/mlavailRDratmodels.shtml), were used as a model of RP. All animals were bred in a colony at the University of Alicante and maintained under controlled humidity (60%), temperature (23 ± 1ºC) and photoperiod (LD 12:12) conditions. Light was provided by two fluorescent lamps, with an intensity of 350-400 lux at cage level. Dry food and water were made available *ad libitum*. All animals were handled in accordance with current regulations for the use of laboratory animals (NIH, ARVO and European Directive 2010/63/UE) in order to minimize animal suffering and limit the numbers used for the experiments.

HU210, purchased from Tocris (Tocris Bioscience, Bristol, UK), was resuspended to stock concentration (5 mg/ml) in ethanol and refrigerated at −20℃ until administration. After being diluted in physiological saline (0.9% NaCl), HU210 was administered at 100 μg/kg (i.p.) three times a week from P24 to P90, when P23H line 3 rats can be considered to have undergone extensive retinal degeneration (http://www.ucsfeye.net/mlavailRDratmodels.shtml) (Fernandez-Sanchez et al., 2012a; Fernandez-Sanchez et al., 2012b; Fernandez-Sanchez et al., 2011). Untreated animals received the same volume of saline at the same time points. In order to adjust the amount of HU210 and vehicle administered, the animal body weight was measured before each drug injection.

2.2. ERG recordings

Scotopic ERGs were performed at P30, P60 and P90, at least 24 h after the last administration of HU210. Following overnight dark adaptation, animals were prepared for bilateral ERG recording under dim red light. Animals were anesthetized by i.p. injection of a ketamine (100 mg/kg) plus xylazine (4 mg/kg) solution, and maintained on a heating pad at 38 ℃. Pupils were dilated by topical application of 1% tropicamide (Alcon Cusí, Barcelona, Spain). A drop of Viscotears 0.2% polyacrylic acid carbomer (Novartis, Barcelona, Spain) was instilled on the cornea to prevent dehydration and allow electrical contact with the recording electrodes. These were DTL fiber electrodes with an X-Static silver-coated nylon conductive strand, from Sauquoit Industries (Scranton, PA). A 25-gauge platinum needle inserted under the scalp between the eyes served as the reference electrode. A gold electrode was placed in the mouth and served as ground. Anesthetized animals were placed in a Faraday cage and all experiments were performed in absolute darkness. Scotopic flash-induced ERG responses were recorded from both eyes in response to light stimuli produced by a Ganzfeld stimulator. Light stimuli were presented for 10 ms at 11 different increasing luminances (ranging from -5.2 to 0 log cd·s/m^{-2}). Three to ten consecutive recordings were averaged for each light presentation. The interval between light flashes was 10 s for dim flashes (-5.2 to -1.4 log cd·s/m^{-2}) and up to 20 s for the higher luminances (-0.8 to 0 log cd·s/m^{-2}). The ERG signals were amplified and band-pass filtered (1-1000 Hz, without notch filtering) using a DAM50 data acquisition board (World Precision Instruments, Aston, UK). Stimulus presentation and data acquisition (4 kHz) were performed using a PowerLab system (AD Instruments, Oxfordshire, UK). Recordings were saved on a computer and analyzed off-line. The amplitude of the a-wave was

measured from the baseline at 10 ms after the onset of the light stimulus, a point before the intrusion of the b-wave. The amplitude of the b-wave was measured from the trough of the a-wave to the peak of the b-wave. Thresholds were defined as the minimal luminance required to reach the criterion amplitude of 10 µV, calculated via curve-fitting (three-parameter sigmoid function) of the luminance-response curve obtained for each series of stimuli. Latency (time-to-peak) was measured from stimulus onset to the a-wave trough and b-wave peak.

2.3. Retinal sections

Animals were sacrificed in the morning by administration of a lethal dose of pentobarbital. After marking the dorsal margin of the limbus with a suture, eyes were enucleated and fixed in 4% (w/v) paraformaldehyde during 1 h at room temperature. After being washed in 0.1 M phosphate buffer pH 7.4 (PB), eyes were cryoprotected sequentially in 15, 20 and 30% sucrose. The cornea, lens and vitreous body were removed, and the retinas were processed for vertical sections. For this purpose, they were embedded in OCT and frozen in liquid N_2. Sixteen µm-thick sections were then obtained at -25 ºC, mounted on Superfrost Plus slides (Menzel GmbH & Co KG, Braunschweig, Germany), and air-dried. Before further use, slides were washed 3 times in PB, and then treated with blocking solution (10% normal donkey serum in PB plus 0.5% Triton X-100) for 1 h.

2.4. Retinal immunohistochemistry

For objective comparison, retinas from vehicle- and HU210-treated rats were fully processed in parallel. All primary antibodies used in this work (summarized in Table 1) have been used in several previous studies and have been well characterized by us and other authors regarding specific cell type molecular markers. Sections were subjected to single or double immunostaining overnight at room temperature, with combinations of antibodies for different molecular markers at the dilutions indicated in Table 1, in PB containing 0.5% Triton X-100. Subsequently, Alexa Fluor 488 (green)-conjugated anti-rabbit IgG and/or Alexa Fluor 555 (red)-conjugated anti-mouse IgG donkey secondary antibodies from Molecular Probes (Eugene, OR) were applied at a 1:100 dilution for 1 h. The sections were finally washed in PB, mounted in Citifluor (Citifluor Ltd; London, UK) and coverslipped for viewing under laser-scanning confocal microscopy on a Leica TCS SP2 system (Wetzlar, Germany). Immunohistochemical controls were performed by omission of either the primary or secondary antibodies. Final images from control and experimental subjects were processed in parallel using the Adobe Photoshop 10 software (Adobe Systems Inc., San Jose, CA). Unless otherwise indicated, all the images analyzed were collected from the central area of the retina, close to the optic nerve.

2.5. Morphometric analysis

Five animals per group were examined. For measurements of the outer nuclear layer (ONL) thickness, a nuclear stain (Hoechst; Sigma, Milwaukee, WI) was added at 1 μg/ml to at least 4 sections from each animal containing the optic nerve and both temporal and nasal ora serratas. Counting of

photoreceptor rows was performed each 0.5 mm from the optic nerve toward each ora serrata. The number of photoreceptor rows was the average of three measurements counting rows of nuclei of photoreceptor cells. For quantification of the relative number of synaptic ribbons in the OPL, we counted the number of Bassoon-immunoreactive puncta in 2 retinal sections from each animal containing the optic nerve and both temporal and nasal ora serratas. Measurements were performed close to the optic nerve, and at 2 and 4 mm from the optic nerve toward each ora serrata. Total length of cones was measured using γ-transducin stained retinal sections. Measurements were performed in the central retina, temporal and nasal, close to the optic nerve, in at least 5 cones from each animal. For evaluation of the ON-rod bipolar cells integrity, we measured the intensity of PKC-α immunoreactivity using the ImageJ software. Fluorescence intensity values were obtained in each animal from 2 pictures of central retinal sections, temporal and nasal, close to the optic nerve. Preservation of photoreceptor presynaptic terminals was evaluated by measuring the relative area of synaptophysin immunostaining in the OPL (μm^2 of positive staining per mm of retinal section). Measurements were performed in each animal from 2 pictures of central retinal sections, temporal and nasal, close to the optic nerve. All quantifications were done in a blinded fashion by multiple experienced observers.

2.6. Statistical analysis

Statistical analyses were performed using SPSS 18.0 software (IBM Armonk, NY). A repeated measures factorial analysis of variance (MANOVA) was performed to evaluate the effects of the treatment (vehicle *vs*. HU210) on

ERG responses throughout the experimental stages (P30, P60 and P90), as well as the interactions among them. When a 0.05 level of significance was found, post hoc pairwise comparisons using Bonferroni's test were made. Normal distributions and homogeneity of variance were found for all analyzed categories. A paired Student's *t*-test was used to evaluate morphological parameters. A regression analysis was performed to establish the relationship between retinal function (by means of the maximum amplitudes of scotopic a- and b-waves) and ONL thickness (taken as an indicator of the number of photoreceptors in the retina). p values less than 0.05 were considered statistically significant. Data were plotted as the mean ± standard error of the mean (SEM).

3. Results

3.1. HU210 preserves retinal responsiveness

In order to evaluate the effect of HU210 on the functional activity of the retina in P23H rats, scotopic flash-induced ERG responses were recorded in vehicle- and HU210-treated animals (n = 6 and n = 5, respectively). As shown in Fig. 1, ERG responsiveness was less deteriorated in P23H rats treated with HU210 (P24 to P90), as compared to vehicle-administered P23H rats. The maximum amplitudes recorded for a-waves at P60 and P90 under scotopic conditions were higher in HU210-treated animals than those recorded in untreated animals (ANOVA, Bonferroni's test, $p < 0.05$ in both cases; Fig. 1A, 1C, 1D). Mean b-wave responses were higher in HU210-treated P23H rats, as compared to vehicle-administered animals, at P30, P60 and P90 (ANOVA, Bonferroni's test, $p < 0.001$ in all cases; Fig. 1A-D). The highest differences in a- and b-wave amplitudes between HU210 and vehicle-administered P23H rats were observed at P90, when the maximum scotopic a-wave (a-max) and b-wave (b-max) amplitude recorded in treated animals resulted, respectively, 71% and 70% higher than that recorded in untreated animals. Thresholds in HU210-treated animals, compared with untreated rats, were lower for scotopic b-waves at P90 (ANOVA, Bonferroni's test, $p < 0.05$; -5.4 ± 0.2 log cd·s/m^2 *vs*. -4.9 ± 0.2 log cd·s/m^2; Fig. 1D). The mean latency of the scotopic a- and b-waves was lower in HU210-treated P23H rats, as compared to vehicle-administered animals, at P60 (ANOVA, Bonferroni's test, $p < 0.01$ in both cases; 26.0 ± 0.6 ms *vs*. 29.9 ± 1.3 ms for a-max, 61.3 ± 1.5 ms *vs*. 66.4 ± 1.2 ms for b-max) and P90 (ANOVA, Bonferroni's test, $p < 0.01$ in both cases; 23.0 ± 1.0 ms *vs*. 29.7 ± 2.1 ms for a-max, 64.2 ± 3.0 ms *vs*. 71.9 ± 3.2 ms for b-max).

3.2. HU210 slows photoreceptor degeneration

To assess the protective action of HU210 on photoreceptors, we analyzed the thickness of the ONL in each retina at P90. Figure 2 shows vertical sections and magnifications of retinas from a P23H rat treated with HU210 (Fig. 2B) or vehicle (Fig. 2A). Few rows of photoreceptor cell bodies could be observed in the ONL of the vehicle-administered rats, as compared with the rows present in the retina of the HU210-treated P23H animals. Because retinal degeneration in untreated P23H rats was not homogeneous throughout the retina, we measured the effects of HU210 in different retinal areas, from temporal to nasal. We found that ONL thickness was greater in HU210-treated rats (n = 5) than in untreated animals (n = 5) in all examined areas (Student's *t*-test, $p < 0.01$; Fig. 3A). On average, the mean number of photoreceptor rows in HU210-treated P23H rats was 40% higher than observed in vehicle-administered P23H rats (2.6 ± 0.2 µm *vs*. 1.8 ± 0.2 µm; Fig. 3A). The mean number of rows of photoreceptor cell bodies found in HU210- and vehicle-administered rat retinas positively correlated with the maximum scotopic ERG b-wave amplitude recorded for each animal at P90 ($p < 0.01$).

We next explored whether the conservation of photoreceptor number was accompanied by a preservation of synaptic connectivity in the OPL. To this end, we used antibodies against bassoon, a protein constituent of synaptic ribbons present in both rod spherules and cone pedicles in the OPL (Cuenca et al., 2004). Few bassoon-immunopositive spots were found at the OPL level in P23H untreated rats, as compared with the number of immunoreactive puncta present in the retina of HU210-treated animals (Fig. 7E, 7F; arrows). Since

retinal degeneration was not homogeneous throughout the retina in P23H rats, we measured the relative number of positively stained ribbons in different retinal areas, from temporal to nasal (Figure 3B). We found that the mean number of Bassoon-immunoreactive puncta in HU210-treated P23H rats was 25% higher (Student's *t*-test, $p < 0.01$) than observed in untreated animals (32.5 ± 2.6 *vs*. 26.0 ± 2.3 stained synaptic ribbons/100µm, n = 5 in both cases; Fig. 3B), indicating that the presynaptic contact elements between photoreceptors and bipolar or horizontal cells were at least partially preserved.

3.3. HU210 preserves photoreceptor morphology

In order to evaluate whether HU210-treatment was able to preserve the morphology of photoreceptors, we examined the staining pattern of antibodies against recoverin, a marker for rods, cones and two bipolar cell subtypes (Cuenca et al., 2004), rhodopsin, which stains rod outer segments (Pinilla et al., 2007), and γ-transducin, a marker for cones (Cuenca et al., 2004). Longer rod inner and outer segments were observed for HU210-treated P23H rats (Fig. 4C) than for vehicle-administered animals (Fig. 4B), where rod degeneration was evident to a greater degree. Drastic changes with age were also observed in the cone photoreceptors of vehicle-administered P23H rats. At P90, their outer segments were both short and swollen and very small in size (Fig. 4E, 4H). The axons were also absent and pedicles emerged directly from the cone cell bodies. In contrast, the typical cone shape can be observed in HU210-treated P23H rats (Fig. 4F, 4I), where outer and inner segments were clearly identified (Fig. 4I; arrows), and axon and pedicle morphology were preserved (Fig. 4I; arrowheads). Mean length of cones in both treated and untreated P23H rats

was smaller than that observed in SD rats (Student's *t*-test, $p < 0.01$ in both cases; Fig. 3C). However, HU210-treated P23H rat retinas showed cone photoreceptors 50% longer than in untreated P23H rat retinas (Student's *t*-test, $p < 0.05$; Fig. 3C).

3.4. HU210 preserves bipolar cells and their synaptic contacts in both plexiform layers

Two bipolar cell subtypes are labeled with antibodies against recoverin (Cuenca et al., 2004): type 8 ON-cone bipolar cells, with weakly immunoreactive cell bodies located near the OPL and a diffuse plexus of axons terminating in strata S4-S5 of the inner plexiform layer (IPL) (Fig. 4A-4C; arrows), and type 2 OFF-cone bipolar cells, with strongly immunoreactive cell bodies located in the middle of the inner nuclear layer (INL) and a dense continuous plexus in strata S1 and S2 of the IPL (Fig. 4A-4C; arrowheads) (Cuenca et al., 2004). On the other hand, γ-transducin antibodies immunostain some types of cone bipolar cells in the rat retina, whose axon terminals are located in all strata of the IPL (Fig. 4D-4I) (Martinez-Navarrete et al., 2011). In HU210-treated rats, bipolar cells immunostained with antibodies against both recoverin and γ-transducin showed (Fig. 4C, 4F) more immunoreactivity and a more complex plexus in the IPL, than that observed in untreated animals (Fig. 4B, 4E).

ON-rod bipolar cells are labeled with antibodies against the α isoform of protein kinase C (PKC-α) (Cuenca et al., 2004). In the rat retina, dendritic terminals of ON-rod bipolar cells establish connections with rod spherules through a large dendritic arbor in the OPL, and their axons ran into the IPL,

each one ending in a bulbous axon terminal in the S5 stratum (Fig. 5). In the retinas of vehicle-administered P23H rats, rod bipolar cells at P90 showed few cell bodies and a retraction of their dendrites (Fig. 5B, 5E). Dendritic branches were scarce, and some cells had virtually no dendrites whatsoever. The number of immunopositive cells appeared to decrease, and their cell bodies were not aligned in the orderly fashion found in wild-type rats (Fig. 5A, 5D). Moreover, a loss of complexity and inmunoreativity can be obseved in the axon terminals of these cells (Cuenca et al., 2004). By contrast, in P23H HU210-treated animals, bipolar cell dendrites were preserved (Fig. 5C, 5F; arrowheads), and the loss of cell bodies was not so extensive. Increased PKC-α imnunoreactivity and larger bulbous axon terminals, with lateral terminal varicosities, were found in central and peripheral retina of HU210-treated rats (Fig. 5C, 5F), as compared with untreated animals (Fig. 5B, 5E). Integrity of ON-rod bipolar cells was evaluated by measuring in the central retina of each experimental group the relative intensity of PKC-α immunoreactivity. As shown in Fig. 3D, ON-rod bipolar cells immunoreactivity in SD rats was significantly greater (Student's *t*-test, $p < 0.05$) than that obtained in untreated P23H rats (58.3% with respect to SD), but not with respect to measured in HU210-treated animals (72.6% of the value in SD).

3.5. HU210 preserves photoreceptor axon terminals and their synaptic contacts with bipolar cells

Given that photoreceptor morphology was preserved in HU210-treated rats, we tested whether photoreceptor presynaptic terminals were protected by HU210 treatment. To this end, we performed staining for synaptophysin (SYP), a presynaptic-vesicle marker present throughout the axon terminals of cones

and rods (Fernandez-Sanchez et al., 2011). GNB3 antibody was used to stain ON-bipolar cells (Fernandez-Bueno et al., 2012). In 3-month-old untreated P23H rats, only an isolated immunoreactive punctate structure for SYP staining was found, indicating loss of photoreceptor axon terminals and giving the OPL the appearance of a discontinuous plexus (Fig. 6B, 6E; arrows). In the remaining cones of peripheral retina, mislocated SYP staining was found along the whole cell, from axon terminals to outer segments (Fig. 6E; arrowheads). By contrast, in HU210-treated P23H rats, a continuous strip of labeled photoreceptor terminals could be observed (Fig. 6C, 6F; arrows), indicating photoreceptor terminal preservation. Double staining for SYP and GNB3 revealed synaptic contacts between rod spherules (labeled for SYP) and the dendritic tips of ON-bipolar cells (labeled for GNB3) in HU210-treated animals (Fig. 6C, 6F). In comparison, fewer of such contacts were observed in vehicle-administered P23H rats (Fig. 6B, 6E). For quantification of these effects, we measured the relative area of SYP immunostaining in the OPL (surface of positive staining per mm of retinal section). As shown in Fig. 3E, photoreceptor axon terminals area in HU210-treated P23H rats was smaller (Student's *t*-test, $p < 0.01$) than that measured in SD rats (35.1%), but significantly higher (Student's *t*-test, $p < 0.01$) than that obtained in untreated P23H rats (18,1% with respect to SD).

3.6. HU210 prevents loss of horizontal cell dendrites and their synaptic contacts with photoreceptors

Horizontal cell bodies are located in the outermost INL of the retina and establish connections with both rod and cone photoreceptors. The only

horizontal cell subtype described in the rat retina can be identified using antibodies against calbindin. In wild-type rats, calbindin labeling reveals a punctate staining of dendritic arborization protruding from horizontal cell bodies and connecting with cone axon terminals, together with thin tangential axonal elongations in the OPL, ending in an extensive arborization connecting with rods (Fig. 7A, arrows). In 3-month-old P23H rats, a retraction and loss of horizontal cell dendritic tips was found (Fig. 7B; arrows), concomitantly with the decrease of stained photoreceptor rows. By contrast, in HU210-treated rat retinas, a higher number of horizontal cell bodies and terminals could be observed (Fig. 7C; arrows).

To explore whether preservation of the dendritic arborization in horizontal cells correlated with preservation of synaptic connectivity in the OPL, we used antibodies against bassoon. Typical bassoon-immunoreactive spots were observed, with a horseshoe morphology corresponding to rod spherules (Fig. 7D-7F; arrows). Double labeling with antibodies against bassoon and calbindin showed numerous pairings between photoreceptor axons and horizontal cell terminals in HU210-treated animals (Fig. 7I; arrows) as compared to fewer contacts observed in untreated P23H rats (Fig. 7H; arrows). These data indicate a preserving effect of HU210 on synaptic contacts between photoreceptors and horizontal cells.

4. Discussion

The present study demonstrates that systemic administration of the cannabinoid HU210 is capable of preserving retinal structure and function in homozygous P23H transgenic rats, a model of autosomal dominant RP. This is the first time that cannabinoid therapy has been assayed in RP. We have focused our study not only on photoreceptor morphology and function, but also on the secondary effects on photoreceptor connectivity and the structure of inner retinal cell layers. The slow retinal degeneration that takes place in P23H line 3 rats (Cuenca et al., 2004; Pinilla et al., 2005) makes this animal model closer to the human condition than other P23H lines and genetic mouse models, thus giving our results additional clinical relevance.

In this study, we found that HU210 therapy in P23H rats ameliorated the loss of both rods and cones characteristic of these animals and preserved their morphology, as evidenced by specific immunostaining of both photoreceptor cell types. Their preservation was in concordance with the higher amplitudes, as well as the lower thresholds and latencies, of scotopic a- and b-waves found in HU210-treated as compared to untreated animals. In fact, the increases in the ONL thickness were significantly correlated with the maximum amplitudes of scotopic b-waves at P90. These results agree with those of our previous studies evaluating the neuroprotective effects of antioxidant and antiapoptotic agents in P23H rats (Fernandez-Sanchez et al., 2012a; Fernandez-Sanchez et al., 2012b; Fernandez-Sanchez et al., 2011; Lax et al., 2011). In this study we have not included photopic ERGs, due to the low amplitude of the ERG responses at P90.

Previous studies have demonstrated that in the 23H rat model cones degenerate secondarily to rods (Garcia-Ayuso et al., 2013). Thus, morphological and functional state of cones depends of the survival of rods and, therefore, of the state of the degenerative process. In our results, regardless the neuroprotective effect of HU210 on retinal photoreceptors, P23H rats showed a significant loss of both rod and cones, as compared to wild-type animals. Accordingly, we can assume that the state of degeneration of these retinas was relatively advanced, as compared with shown in previous studies (Cuenca et al., 2004). Various mechanisms of cone-rod dependence for survival have been postulated: rods secrete an essential survival factor for cones (Leveillard et al., 2004); rod loss causes oxidative damage to cones (Stone et al., 1999); retinal and choroidal degenerative changes impede normal photoreceptor nutrition (Marc and Jones, 2003; Marc et al., 2003); and degenerating rods generate a toxin that reaches cones by gap junctions, causing their death (Ripps, 2002).

In addition to the preventive effects of HU210 on photoreceptor number, morphology and function, P23H HU210-treated rats experienced improved connectivity between photoreceptors and their postsynaptic neurons, i.e., horizontal and bipolar cells. Both presynaptic and postsynaptic elements, as well as synaptic contacts between photoreceptors and bipolar and horizontal cells, were preserved in HU210-treated P23H rats. Furthermore, in these rats, the number of both rod bipolar and horizontal cell bodies, as well as the density of their dendritic terminals, was higher than in vehicle-administered rats. These results strongly indicate that the effect of HU210 on retinal morphology and function is not cell specific and, therefore, extends not only to photoreceptors but also to other retinal cell types. Another interesting possibility is that the

preservation of the photoreceptor population prevents the occurrence of secondary degenerative changes in their postsynaptic neurons, thereby preventing the remodeling of the entire retinal circuitry (Jones and Marc, 2005; Marc et al., 2003).

The neuroprotective effects of HU210 on retinal degeneration might be exerted through the endocannabinoid system. Endocannabinoids have been shown to provide neuroprotection against ischemia (Pellegrini-Giampietro et al., 2009), traumatic brain injury (Shohami et al., 1993), inflammation-induced neuronal damage (Eljaschewitsch et al., 2006) and neurotoxicity (van der Stelt and Di Marzo, 2005). The proposed mechanisms for these actions include blockade of microglial activation (Ramirez et al., 2005), increase in neurotrophic factors (Khaspekov et al., 2004), reduction of calcium influx (Nadler et al., 1993) and antioxidant activity (El-Remessy et al., 2003), among others. Some of these mechanisms are mediated by the CB1 receptor (e.g. inhibition of glutamate release, decrease in cytosolic free Ca^{2+} concentration), whereas others implicate CB2 receptors, mainly through a series of glia-dependent anti-inflammatory actions (Fernandez-Ruiz et al., 2007). HU210 has similar affinity for CB1 and CB2 receptors (Pertwee, 1999), whose immunoreactivity has been found in the retina of rodents and primates (Bouskila et al., 2012; Bouskila et al., 2013; Cecyre et al., 2013; Lopez et al., 2011; Straiker et al., 1999a; Yazulla, 2008; Yazulla et al., 1999). Furthermore, evidence of cannabinoid function has been provided in ganglion cells (Lalonde et al., 2006; Middleton and Protti, 2011), bipolar cells (Straiker et al., 1999b; Yazulla et al., 2000) and photoreceptors (Fan and Yazulla, 2003; Straiker and Sullivan, 2003). HU210 has been shown to be 100 to 800 times more potent than THC (Ottani and

Giuliani, 2001), having a slightly longer duration of action than the analog natural cannabinoid (Little et al., 1989; Ottani and Giuliani, 2001). Furthermore, neuroprotective effects of HU210 have been demonstrated in Alzheimer's disease (Ramirez et al., 2005), Parkinson's disease (Walsh et al., 2010), ischemic damage (Leker et al., 2003) and neurotoxicity (Pope et al., 2010; Rubio et al., 2011), among others.

Some of the neuroprotective mechanisms attributable to cannabinoids are independent of CB receptors. Previous reports have described the neuroprotective effects of cannabinoids via blocking ROS (Hampson et al., 1998; Hampson et al., 2000). In this sense, it has been demonstrated that antioxidant receptor-independent cannabinoids provide neuroprotection in Parkinson's disease (Garcia-Arencibia et al., 2007). HU210 has been found to be a potent lipophilic antioxidant, and it behaves as a protective agent against oxidative stress in neuronal cell lines (Marsicano et al., 2002). Moreover, antioxidant effects of HU210 have been evidenced in neural damage in diabetic mice (Dagon et al., 2007).

From our results, we are not able to deduce the mechanisms involved in the neuroprotective actions of HU210 in the retina of P23H rats. Future studies using specific agonists for CB1 and CB2 receptors and antagonists for these receptors are necessary to determine if these effects are mediated by CB1 and/or CB2 receptors and, in that case, what is/are the receptor(s) involved in these actions. These studies might also establish whether HU210-neuroprotection result from a direct effect on photoreceptors or, instead, by an indirect effect through glia-dependent actions. Future studies are also needed

to establish the dose and schedule in which HU210 may exert its greatest neuroprotective effect.

In RP disease, despite the use of therapies aimed at preventing cell death, the loss of photoreceptors in number and function usually leads to a dramatic remodeling of retinal circuits that would probably further compromise the transmission of visual information (Cuenca et al., 2004). In this context, the use of therapies such as cannabinoids, effective not only in preserving photoreceptor loss but also in slowing the degeneration of inner retinal layers, may be especially interesting in combination with other therapies based on the transplantation of stem cells, anti-inflammatory or anti-apoptotic agents, and artificial chips, among others.

Acknowledgements

This research was supported by grants from the Spanish Ministry of Economy and Competitiveness (BFU2012-36845), Instituto de Salud Carlos III (RETICS RD12/0034/0010), Universidad de Alicante (UA2010-48536273), and the Organización Nacional de Ciegos Españoles (ONCE).

References

Ahuja, P., Caffe, A.R., Ahuja, S., Ekstrom, P., van Veen, T., 2005. Decreased glutathione transferase levels in rd1/rd1 mouse retina: replenishment protects photoreceptors in retinal explants. Neuroscience 131, 935-943.

Berson, E.L., Rosner, B., Sandberg, M.A., Dryja, T.P., 1991. Ocular findings in patients with autosomal dominant retinitis pigmentosa and a rhodopsin gene defect (Pro-23-His). Arch Ophthalmol 109, 92-101.

Berson, E.L., Rosner, B., Sandberg, M.A., Hayes, K.C., Nicholson, B.W., Weigel-DiFranco, C., Willett, W., 1993. A randomized trial of vitamin A and vitamin E supplementation for retinitis pigmentosa. Arch Ophthalmol 111, 761-772.

Bouskila, J., Burke, M.W., Zabouri, N., Casanova, C., Ptito, M., Bouchard, J.F., 2012. Expression and localization of the cannabinoid receptor type 1 and the enzyme fatty acid amide hydrolase in the retina of vervet monkeys. Neuroscience 202, 117-130.

Bouskila, J., Javadi, P., Casanova, C., Ptito, M., Bouchard, J.F., 2013. Muller cells express the cannabinoid CB2 receptor in the vervet monkey retina. J Comp Neurol 521, 2399-2415.

Cayouette, M., Behn, D., Sendtner, M., Lachapelle, P., Gravel, C., 1998. Intraocular gene transfer of ciliary neurotrophic factor prevents death and increases responsiveness of rod photoreceptors in the retinal degeneration slow mouse. J Neurosci 18, 9282-9293.

Cayouette, M., Smith, S.B., Becerra, S.P., Gravel, C., 1999. Pigment epithelium-derived factor delays the death of photoreceptors in mouse models of inherited retinal degenerations. Neurobiol Dis 6, 523-532.

Cecyre, B., Zabouri, N., Huppe-Gourgues, F., Casanova, C., Bouchard, J.F., 2013. Roles of cannabinoid receptors type 1 and 2 on the retinal function of adult mice. Invest Ophthalmol Vis Sci.

Chong, N.H., Alexander, R.A., Waters, L., Barnett, K.C., Bird, A.C., Luthert, P.J., 1999. Repeated injections of a ciliary neurotrophic factor analogue leading to long-term photoreceptor survival in hereditary retinal degeneration. Invest Ophthalmol Vis Sci 40, 1298-1305.

Crandall, J., Matragoon, S., Khalifa, Y.M., Borlongan, C., Tsai, N.T., Caldwell, R.B., Liou, G.I., 2007. Neuroprotective and intraocular pressure-lowering effects of (-)Delta9-tetrahydrocannabinol in a rat model of glaucoma. Ophthalmic Res 39, 69-75.

Cuenca, N., Pinilla, I., Sauve, Y., Lu, B., Wang, S., Lund, R.D., 2004. Regressive and reactive changes in the connectivity patterns of rod and cone pathways of P23H transgenic rat retina. Neuroscience 127, 301-317.

Dagon, Y., Avraham, Y., Link, G., Zolotarev, O., Mechoulam, R., Berry, E.M., 2007. The synthetic cannabinoid HU-210 attenuates neural damage in diabetic mice and hyperglycemic pheochromocytoma PC12 cells. Neurobiol Dis 27, 174-181.

Doonan, F., Cotter, T.G., 2004. Apoptosis: a potential therapeutic target for retinal degenerations. Curr Neurovasc Res 1, 41-53.

Dryja, T.P., McEvoy, J.A., McGee, T.L., Berson, E.L., 2000. Novel rhodopsin mutations Gly114Val and Gln184Pro in dominant retinitis pigmentosa. Invest Ophthalmol Vis Sci 41, 3124-3127.

Dryja, T.P., McGee, T.L., Reichel, E., Hahn, L.B., Cowley, G.S., Yandell, D.W., Sandberg, M.A., Berson, E.L., 1990. A point mutation of the rhodopsin gene in one form of retinitis pigmentosa. Nature 343, 364-366.

El-Remessy, A.B., Khalil, I.E., Matragoon, S., Abou-Mohamed, G., Tsai, N.J., Roon, P., Caldwell, R.B., Caldwell, R.W., Green, K., Liou, G.I., 2003. Neuroprotective effect of (-)Delta9-tetrahydrocannabinol and cannabidiol in N-methyl-D-aspartate-induced retinal neurotoxicity: involvement of peroxynitrite. Am J Pathol 163, 1997-2008.

Eljaschewitsch, E., Witting, A., Mawrin, C., Lee, T., Schmidt, P.M., Wolf, S., Hoertnagl, H., Raine, C.S., Schneider-Stock, R., Nitsch, R., Ullrich, O., 2006. The endocannabinoid anandamide protects neurons during CNS inflammation by induction of MKP-1 in microglial cells. Neuron 49, 67-79.

Fan, S.F., Yazulla, S., 2003. Biphasic modulation of voltage-dependent currents of retinal cones by cannabinoid CB1 receptor agonist WIN 55212-2. Vis Neurosci 20, 177-188.

Fernandez-Bueno, I., Fernandez-Sanchez, L., Gayoso, M.J., Garcia-Gutierrez, M.T., Pastor, J.C., Cuenca, N., 2012. Time course modifications in organotypic culture of human neuroretina. Exp Eye Res 104, 26-38.

Fernandez-Ruiz, J., Garcia, C., Sagredo, O., Gomez-Ruiz, M., de Lago, E., 2010. The endocannabinoid system as a target for the treatment of neuronal damage. Expert Opin Ther Targets 14, 387-404.

Fernandez-Ruiz, J., Romero, J., Velasco, G., Tolon, R.M., Ramos, J.A., Guzman, M., 2007. Cannabinoid CB2 receptor: a new target for controlling neural cell survival? Trends Pharmacol Sci 28, 39-45.

Fernandez-Sanchez, L., Lax, P., Esquiva, G., Martin-Nieto, J., Pinilla, I., Cuenca, N., 2012a. Safranal, a saffron constituent, attenuates retinal degeneration in P23H rats. PLoS One 7, e43074.

Fernandez-Sanchez, L., Lax, P., Isiegas, C., Ayuso, E., Ruiz, J.M., de la Villa, P., Bosch, F., de la Rosa, E.J., Cuenca, N., 2012b. Proinsulin slows retinal degeneration and vision loss in the P23H rat model of retinitis pigmentosa. Hum Gene Ther 23, 1290-1300.

Fernandez-Sanchez, L., Lax, P., Pinilla, I., Martin-Nieto, J., Cuenca, N., 2011. Tauroursodeoxycholic acid prevents retinal degeneration in transgenic P23H rats. Invest Ophthalmol Vis Sci 52, 4998-5008.

Garcia-Arencibia, M., Gonzalez, S., de Lago, E., Ramos, J.A., Mechoulam, R., Fernandez-Ruiz, J., 2007. Evaluation of the neuroprotective effect of cannabinoids in a rat model of Parkinson's disease: importance of antioxidant and cannabinoid receptor-independent properties. Brain Res 1134, 162-170.

Garcia-Ayuso, D., Ortin-Martinez, A., Jimenez-Lopez, M., Galindo-Romero, C., Cuenca, N., Pinilla, I., Vidal-Sanz, M., Agudo-Barriuso, M., Villegas-Perez, M.P., 2013. Changes in the Photoreceptor Mosaic of P23H-1 Rats During Retinal Degeneration: Implications for Rod-Cone Dependent Survival. Invest Ophthalmol Vis Sci 54, 5888-5900.

Garcia-Ayuso, D., Salinas-Navarro, M., Agudo, M., Cuenca, N., Pinilla, I., Vidal-Sanz, M., Villegas-Perez, M.P., 2010. Retinal ganglion cell numbers and delayed retinal ganglion cell death in the P23H rat retina. Exp Eye Res 91, 800-810.

Green, E.S., Rendahl, K.G., Zhou, S., Ladner, M., Coyne, M., Srivastava, R., Manning, W.C., Flannery, J.G., 2001. Two animal models of retinal degeneration are rescued by recombinant adeno-associated virus-mediated production of FGF-5 and FGF-18. Mol Ther 3, 507-515.

Hampson, A.J., Grimaldi, M., Axelrod, J., Wink, D., 1998. Cannabidiol and (-)Delta9-tetrahydrocannabinol are neuroprotective antioxidants. Proc Natl Acad Sci U S A 95, 8268-8273.

Hampson, A.J., Grimaldi, M., Lolic, M., Wink, D., Rosenthal, R., Axelrod, J., 2000. Neuroprotective antioxidants from marijuana. Ann N Y Acad Sci 899, 274-282.

Hartong, D.T., Berson, E.L., Dryja, T.P., 2006. Retinitis pigmentosa. Lancet 368, 1795-1809.

Illing, M.E., Rajan, R.S., Bence, N.F., Kopito, R.R., 2002. A rhodopsin mutant linked to autosomal dominant retinitis pigmentosa is prone to aggregate and interacts with the ubiquitin proteasome system. J Biol Chem 277, 34150-34160.

Jones, B.W., Marc, R.E., 2005. Retinal remodeling during retinal degeneration. Exp Eye Res 81, 123-137.

Kaushal, S., Khorana, H.G., 1994. Structure and function in rhodopsin. 7. Point mutations associated with autosomal dominant retinitis pigmentosa. Biochemistry 33, 6121-6128.

Khaspekov, L.G., Brenz Verca, M.S., Frumkina, L.E., Hermann, H., Marsicano, G., Lutz, B., 2004. Involvement of brain-derived neurotrophic factor in cannabinoid receptor-dependent protection against excitotoxicity. Eur J Neurosci 19, 1691-1698.

Kolomiets, B., Dubus, E., Simonutti, M., Rosolen, S., Sahel, J.A., Picaud, S., 2010. Late histological and functional changes in the P23H rat retina after photoreceptor loss. Neurobiol Dis 38, 47-58.

Komeima, K., Rogers, B.S., Lu, L., Campochiaro, P.A., 2006. Antioxidants reduce cone cell death in a model of retinitis pigmentosa. Proc Natl Acad Sci U S A 103, 11300-11305.

Lalonde, M.R., Jollimore, C.A., Stevens, K., Barnes, S., Kelly, M.E., 2006. Cannabinoid receptor-mediated inhibition of calcium signaling in rat retinal ganglion cells. Mol Vis 12, 1160-1166.

Lax, P., Otalora, B.B., Esquiva, G., Rol Mde, L., Madrid, J.A., Cuenca, N., 2011. Circadian dysfunction in P23H rhodopsin transgenic rats: effects of exogenous melatonin. J Pineal Res 50, 183-191.

Leker, R.R., Gai, N., Mechoulam, R., Ovadia, H., 2003. Drug-induced hypothermia reduces ischemic damage: effects of the cannabinoid HU-210. Stroke 34, 2000-2006.

Leveillard, T., Mohand-Said, S., Lorentz, O., Hicks, D., Fintz, A.C., Clerin, E., Simonutti, M., Forster, V., Cavusoglu, N., Chalmel, F., Dolle, P., Poch, O., Lambrou, G., Sahel, J.A., 2004. Identification and characterization of rod-derived cone viability factor. Nat Genet 36, 755-759.

Liang, F.Q., Aleman, T.S., ZaixinYang, Cideciyan, A.V., Jacobson, S.G., Bennett, J., 2001. Melatonin delays photoreceptor degeneration in the rds/rds mouse. Neuroreport 12, 1011-1014.

Little, P.J., Compton, D.R., Mechoulam, R., Martin, B.R., 1989. Stereochemical effects of 11-OH-delta 8-THC-dimethylheptyl in mice and dogs. Pharmacol Biochem Behav 32, 661-666.

Lopez, E.M., Tagliaferro, P., Onaivi, E.S., Lopez-Costa, J.J., 2011. Distribution of CB2 cannabinoid receptor in adult rat retina. Synapse 65, 388-392.

Machida, S., Kondo, M., Jamison, J.A., Khan, N.W., Kononen, L.T., Sugawara, T., Bush, R.A., Sieving, P.A., 2000. P23H rhodopsin transgenic rat: correlation of retinal function with histopathology. Invest Ophthalmol Vis Sci 41, 3200-3209.

Marc, R.E., Jones, B.W., 2003. Retinal remodeling in inherited photoreceptor degenerations. Mol Neurobiol 28, 139-147.

Marc, R.E., Jones, B.W., Watt, C.B., Strettoi, E., 2003. Neural remodeling in retinal degeneration. Prog Retin Eye Res 22, 607-655.

Marsicano, G., Moosmann, B., Hermann, H., Lutz, B., Behl, C., 2002. Neuroprotective properties of cannabinoids against oxidative stress: role of the cannabinoid receptor CB1. J Neurochem 80, 448-456.

Martinez-Navarrete, G., Seiler, M.J., Aramant, R.B., Fernandez-Sanchez, L., Pinilla, I., Cuenca, N., 2011. Retinal degeneration in two lines of transgenic S334ter rats. Exp Eye Res 92, 227-237.

McGee Sanftner, L.H., Abel, H., Hauswirth, W.W., Flannery, J.G., 2001. Glial cell line derived neurotrophic factor delays photoreceptor degeneration in a transgenic rat model of retinitis pigmentosa. Mol Ther 4, 622-629.

Mechoulam, R., Feigenbaum, J.J., Lander, N., Segal, M., Jarbe, T.U., Hiltunen, A.J., Consroe, P., 1988. Enantiomeric cannabinoids: stereospecificity of psychotropic activity. Experientia 44, 762-764.

Middleton, T.P., Protti, D.A., 2011. Cannabinoids modulate spontaneous synaptic activity in retinal ganglion cells. Vis Neurosci 28, 393-402.

Musarella, M.A., Macdonald, I.M., 2011. Current concepts in the treatment of retinitis pigmentosa. J Ophthalmol 2011, 753547.

Nadler, V., Mechoulam, R., Sokolovsky, M., 1993. Blockade of 45Ca2+ influx through the N-methyl-D-aspartate receptor ion channel by the non-psychoactive cannabinoid HU-211. Brain Res 622, 79-85.

Nucci, C., Gasperi, V., Tartaglione, R., Cerulli, A., Terrinoni, A., Bari, M., De Simone, C., Agro, A.F., Morrone, L.A., Corasaniti, M.T., Bagetta, G., Maccarrone, M., 2007. Involvement of the endocannabinoid system in retinal damage after high intraocular pressure-induced ischemia in rats. Invest Ophthalmol Vis Sci 48, 2997-3004.

Okoye, G., Zimmer, J., Sung, J., Gehlbach, P., Deering, T., Nambu, H., Hackett, S., Melia, M., Esumi, N., Zack, D.J., Campochiaro, P.A., 2003. Increased expression of brain-derived neurotrophic factor preserves retinal function and slows cell death from rhodopsin mutation or oxidative damage. J Neurosci 23, 4164-4172.

Opere, C.A., Zheng, W.D., Zhao, M., Lee, J.S., Kulkarni, K.H., Ohia, S.E., 2006. Inhibition of potassium- and ischemia-evoked [3H] D-aspartate

release from isolated bovine retina by cannabinoids. Curr Eye Res 31, 645-653.

Ottani, A., Giuliani, D., 2001. Hu 210: a potent tool for investigations of the cannabinoid system. CNS Drug Rev 7, 131-145.

Pellegrini-Giampietro, D.E., Mannaioni, G., Bagetta, G., 2009. Post-ischemic brain damage: the endocannabinoid system in the mechanisms of neuronal death. FEBS J 276, 2-12.

Pertwee, R.G., 1999. Pharmacology of cannabinoid receptor ligands. Curr Med Chem 6, 635-664.

Pertwee, R.G., 2012. Targeting the endocannabinoid system with cannabinoid receptor agonists: pharmacological strategies and therapeutic possibilities. Philos Trans R Soc Lond B Biol Sci 367, 3353-3363.

Pinar-Sueiro, S., Zorrilla Hurtado, J.A., Veiga-Crespo, P., Sharma, S.C., Vecino, E., 2013. Neuroprotective effects of topical CB1 agonist WIN 55212-2 on retinal ganglion cells after acute rise in intraocular pressure induced ischemia in rat. Exp Eye Res 110, 55-58.

Pinilla, I., Cuenca, N., Sauve, Y., Wang, S., Lund, R.D., 2007. Preservation of outer retina and its synaptic connectivity following subretinal injections of human RPE cells in the Royal College of Surgeons rat. Exp Eye Res 85, 381-392.

Pinilla, I., Lund, R.D., Sauve, Y., 2005. Enhanced cone dysfunction in rats homozygous for the P23H rhodopsin mutation. Neurosci Lett 382, 16-21.

Pope, C., Mechoulam, R., Parsons, L., 2010. Endocannabinoid signaling in neurotoxicity and neuroprotection. Neurotoxicology 31, 562-571.

Ramirez, B.G., Blazquez, C., Gomez del Pulgar, T., Guzman, M., de Ceballos, M.L., 2005. Prevention of Alzheimer's disease pathology by cannabinoids: neuroprotection mediated by blockade of microglial activation. J Neurosci 25, 1904-1913.

Reme, C.E., Grimm, C., Hafezi, F., Marti, A., Wenzel, A., 1998. Apoptotic cell death in retinal degenerations. Prog Retin Eye Res 17, 443-464.

Ripps, H., 2002. Cell death in retinitis pigmentosa: gap junctions and the 'bystander' effect. Exp Eye Res 74, 327-336.

Rubio, M., Villain, H., Docagne, F., Roussel, B.D., Ramos, J.A., Vivien, D., Fernandez-Ruiz, J., Ali, C., 2011. Pharmacological activation/inhibition of the cannabinoid system affects alcohol withdrawal-induced neuronal hypersensitivity to excitotoxic insults. PLoS One 6, e23690.

Shohami, E., Novikov, M., Mechoulam, R., 1993. A nonpsychotropic cannabinoid, HU-211, has cerebroprotective effects after closed head injury in the rat. J Neurotrauma 10, 109-119.

Stieger, K., 2010. tgAAG76, an adeno-associated virus delivered gene therapy for the potential treatment of vision loss caused by RPE65 gene abnormalities. Curr Opin Mol Ther 12, 471-477.

Stone, J., Maslim, J., Valter-Kocsi, K., Mervin, K., Bowers, F., Chu, Y., Barnett, N., Provis, J., Lewis, G., Fisher, S.K., Bisti, S., Gargini, C., Cervetto, L., Merin, S., Peer, J., 1999. Mechanisms of photoreceptor death and survival in mammalian retina. Prog Retin Eye Res 18, 689-735.

Straiker, A., Stella, N., Piomelli, D., Mackie, K., Karten, H.J., Maguire, G., 1999a. Cannabinoid CB1 receptors and ligands in vertebrate retina: localization and function of an endogenous signaling system. Proc Natl Acad Sci U S A 96, 14565-14570.

Straiker, A., Sullivan, J.M., 2003. Cannabinoid receptor activation differentially modulates ion channels in photoreceptors of the tiger salamander. J Neurophysiol 89, 2647-2654.

Straiker, A.J., Maguire, G., Mackie, K., Lindsey, J., 1999b. Localization of cannabinoid CB1 receptors in the human anterior eye and retina. Invest Ophthalmol Vis Sci 40, 2442-2448.

van der Stelt, M., Di Marzo, V., 2005. Cannabinoid receptors and their role in neuroprotection. Neuromolecular Med 7, 37-50.

Walsh, S., Gorman, A.M., Finn, D.P., Dowd, E., 2010. The effects of cannabinoid drugs on abnormal involuntary movements in dyskinetic and non-dyskinetic 6-hydroxydopamine lesioned rats. Brain Res 1363, 40-48.

Yazulla, S., 2008. Endocannabinoids in the retina: from marijuana to neuroprotection. Prog Retin Eye Res 27, 501-526.

Yazulla, S., Studholme, K.M., McIntosh, H.H., Deutsch, D.G., 1999. Immunocytochemical localization of cannabinoid CB1 receptor and fatty acid amide hydrolase in rat retina. J Comp Neurol 415, 80-90.

Yazulla, S., Studholme, K.M., McIntosh, H.H., Fan, S.F., 2000. Cannabinoid receptors on goldfish retinal bipolar cells: electron-microscope immunocytochemistry and whole-cell recordings. Vis Neurosci 17, 391-401.

Zogopoulos, P., Vasileiou, I., Patsouris, E., Theocharis, S., 2013. The neuroprotective role of endocannabinoids against chemical-induced injury and other adverse effects. J Appl Toxicol 33, 246-264.

Figure legends

Fig. 1. ERG responsiveness in untreated and HU210-treated P23H rats. (A) Scotopic ERG traces in a untreated and HU210-treated P23H rat at P30, P60 and P90. Units on the left of the panel indicate input flash intensities in log cd·s/m^2. (B-D) Luminance-response curves in untreated (circle) and HU210-treated (square) P23H rats at P30 (B), P60 (C) and P90 (D). Average amplitudes of a-waves were higher in treated animals (n=6) than in untreated P23H rats (n=5) at P60 and P90 (ANOVA, Bonferroni's test, $p < 0.001$). b-waves were also higher in treated rats, as compared to untreated rats, at P30, P60 and P90 (ANOVA, Bonferroni's test, $p < 0.001$). *$p < 0.05$, **$p < 0.001$; ANOVA, Bonferroni's test).

Fig. 2. Assessment of the photoreceptor layer in untreated and HU210-treated P23H rats. Vertical sections and high magnification views from an untreated (A) and HU210-treated (B) P23H rat retina at P90. GNB3 antibody stains ON-bipolar cells (red), whereas synaptophysin labels presynaptic vesicles in both OPL and IPL (green). Nuclei stained with TO-PRO (blue). Animals treated with HU210 display higher number of photoreceptor rows at the retinal ONL than untreated animals. ONL, outer nuclear layer. Scale bar: 1mm; inset: 50 μm.

Fig. 3. Quantification of structural changes in untreated and HU210-treated P23H rats. (A) Average number of photoreceptor rows throughout the naso-temporal axis in untreated (n = 5; circles) and HU210-treated (n = 5; squares) P23H rats at P90. The mean number of photoreceptor rows in HU210-treated P23H rats was 40% higher than observed in untreated rats ($p < 0.001$). (B) Average number of positively stained synaptic ribbons from nasal to temporal retina in untreated (n = 5; black bars) and HU210-treated (n = 5; white bars)

P23H rats. The mean number of Basson-immunoreactive spots was 25% higher in HU210-treated P23H rats, as compared to untreated animals ($p < 0.01$). (C) Average length of cones in the central retina of wild-type rats (Sprague Dawley, SD) (n = 5; grey bar) and P23H rats treated with vehicle (n = 5; black bar) or HU210 (n = 5; white bar). (D) Relative PKC-α immunoreactivity of ON-rod bipolar cells in the central retina of Sprague Dawley rats (SD) (n = 5; grey bar) and P23H rats treated with vehicle (n = 5; black bar) or HU210 (n = 5; white bar). (E) Relative area of SYP immunostaining of photoreceptor axon terminals in the OPL (surface of positive staining per mm of retinal section) of Sprague Dawley rats (SD) (n = 5; grey bar) and P23H rats treated with vehicle (n = 5; black bar) or HU210 (n = 5; white bar). *$p < 0.05$, **$p < 0.001$; Student's t test. ON, optic nerve; OS, ora serrata.

Fig. 4. Photoreceptor cell morphology in untreated and HU210-treated P23H rats. Vertical sections at P90 of retinas from wild-type rats (Sprague Dawley, SD) (A, D, G) and P23H rats treated with vehicle (B, E, H) or HU210 (C, F, I). (A-C) Recoverin-stained (cones and rods; red) and rhodopsin-stained (rod outer segments; green) retinas showing a more profuse degeneration in the vehicle-treated P23H rat (B) than that observed in the HU210-treated P23H rat (C). Besides cones and rods, antibodies against recoverin specifically stained type 8 (arrows) and type 2 (arrowheads) bipolar cells. (D-F) Cone staining for γ-transducin shows smaller cell sizes, and shorter and swollen outer segments in vehicle-treated P23H rats (E) than in HU210-treated P23H rats (F). γ-transducin antibodies also stained some types of cone bipolar cells. Nuclei stained with a nuclear marker (blue). (G-I) High magnification of cone stainings, showing preservation in the HU210-treated P23H rat (I) of cone outer and inner

segments (arrows), and maintenance in this animal of axon and pedicle morphology (arrowheads). All images were collected from the central area of the retina, close to the optic nerve. OS, outer segment; IS, inner segment; ONL, outer nuclear layer; OPL, outer plexiform layer; INL, inner nuclear layer; IPL, inner plexiform layer; GCL, ganglion cell layer; ONF, optic nerve fibers. Scale bar: 20μm.

Fig. 5. ON-rod bipolar cells and their synaptic connectivity in untreated and HU210-treated P23H rats. PKC-α staining of ON-rod bipolar cells in vertical sections at P90 from wild-type rats (Sprague Dawley, SD) (A, D) and P23H rats treated with vehicle (B, E) or HU210 (C, F). Insets show higher magnification images of the bipolar cell dendritic arbors in the OPL. Nuclei stained with nuclear marker (blue). Note that cell bodies and dendrites (arrowheads) were more preserved in HU210-treated P23H rats than in untreated animals, in both central (B, C) and peripheral (E, F) retina. Scale bar: 20 μm and 10 μm (insets).

Fig. 6. Photoreceptor presynaptic terminals in untreated and HU210-treated P23H rats. Vertical sections at P90 of retinas from wild-type rats (Sprague Dawley, SD) (A, D) and P23H rats treated with vehicle (B, E) or HU210 (C, F). GNB3 antibody stains ON-bipolar cells (red), whereas SYP labels presynaptic vesicles of cones and rods (green; arrows). Nuclei stained with nuclear marker (blue). Note that synaptic contacts between photoreceptors and bipolar cells are less deteriorated in HU210-treated P23H rats than in untreated animals, in both central (B, C) and peripheral (E, F) retina. Mislocated SYP staining was found in the soma of remaining cones in peripheral retina of P23H untreated animals (E; arrowheads). Scale bar: 20 μm.

Fig. 7. Horizontal cells and their synaptic contacts in untreated and HU210-treated P23H rats. Vertical sections at P90 of retinas from wild-type rats (Sprague Dawley, SD) (A, D, G) and P23H rats treated with vehicle (B, E, H) or HU210 (C, F, I). Nuclei stained with nuclear marker (blue). (A-C) Horizontal cells labeled with antibodies against calbindin. Note that the number of horizontal cell terminals (arrows) in HU210-treated P23H rats was higher than in vehicle-treated animals. (D-F) Labeling of photoreceptor synaptic ribbons (arrows) with antibodies against bassoon. (G-I) Double immunolabeling for calbindin and bassoon showing a larger number of synaptic contacts (arrows) between photoreceptor and horizontal cells in HU210-treated rats (I) than observed in the untreated P23H rats (H). All images were collected from the central area of the retina, close to the optic nerve. Scale bar: 10 μm.

Table 1. Primary antibodies

Molecular marker	Antibody	Source	Working dilution
Bassoon	Mouse monoclonal (Cuenca et al., 2004)	Stressgen	1:1000
Calbindin D-28K	Rabbit polyclonal (Cuenca et al., 2004)	Swant	1:500
GNB3	Rabbit polyclonal (Fernandez-Bueno et al., 2012)	SIGMA	1:50
PKC (α isoforms)	Rabbit polyclonal (Cuenca et al., 2004)	Santa Cruz Biotechnology	1:100
Recoverin	Mouse monoclonal (Cuenca et al., 2004)	J.F. McGinnis, University of Oklahoma	1:2000
Rhodopsin	Mouse monoclonal (Pinilla et al., 2007)	Chemicon	1:200
Synaptophysin	Mouse, clone SY38 (Fernandez-Sanchez et al., 2011)	Chemicon	1:500
γ-Transducin	Rabbit polyclonal (Cuenca et al., 2004)	Cytosignal	1:200

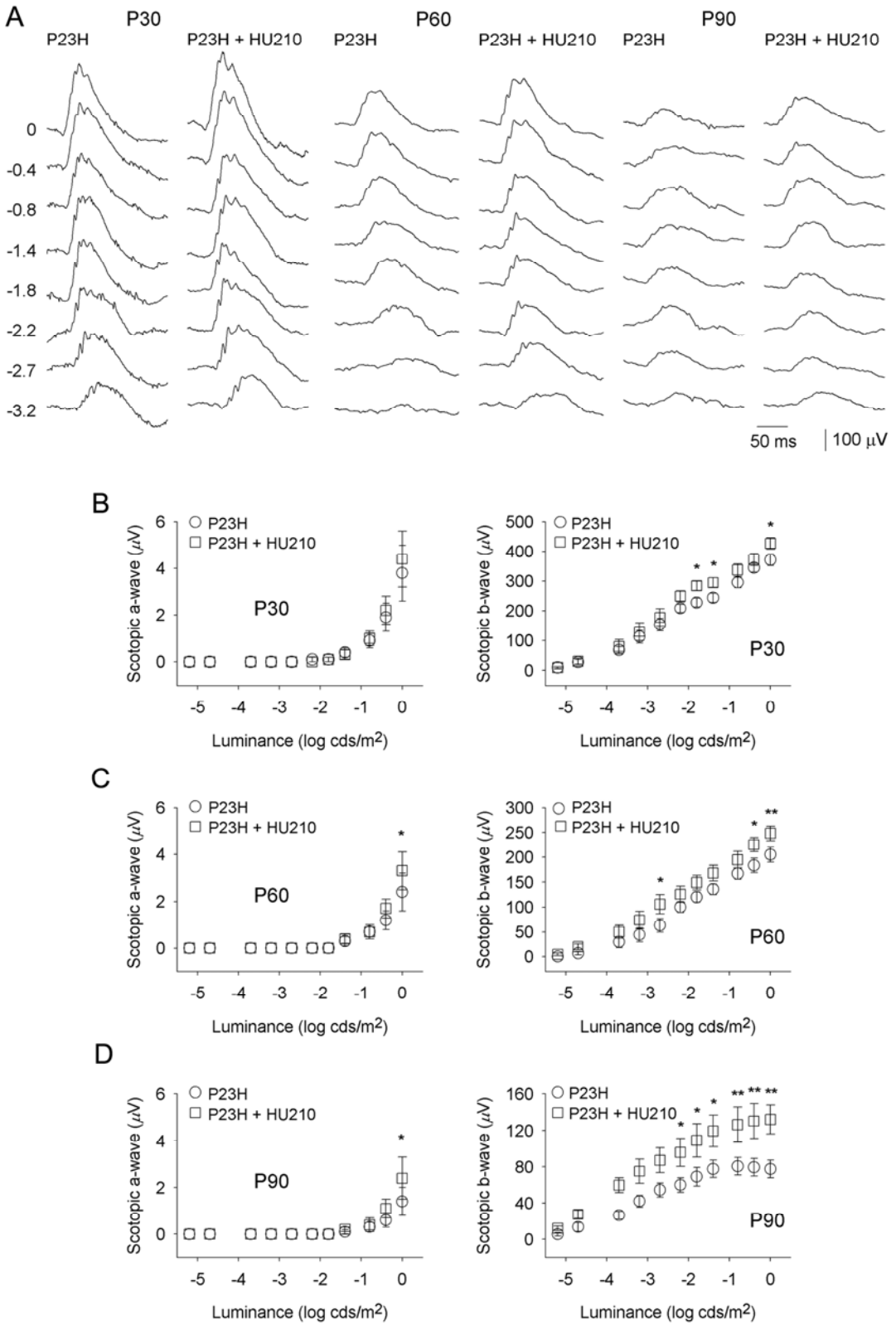
A
P30
P60
P90
P23H
P23H + HU210
P23H
P23H + HU210
P23H
P23H + HU210
0
-0.4
-0.8
-1.4
-1.8
-2.2
-2.7
-3.2
50 ms
100 μV
B
P23H
P23H + HU210
P30
Scotopic a-wave (μV)
Scotopic b-wave (μV)
Luminance (log cds/m2)
C
P60
D
P90

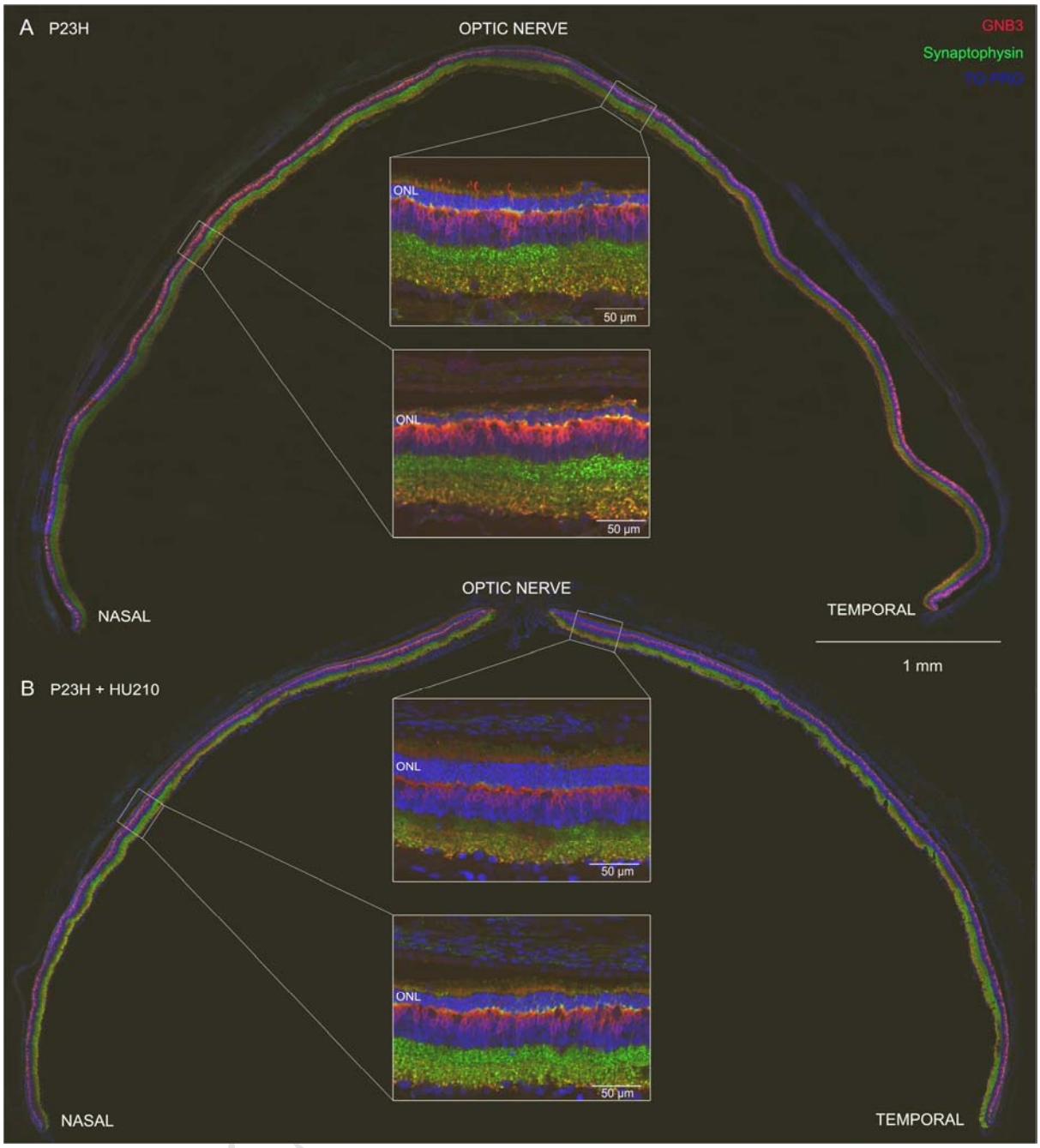
A P23H
OPTIC NERVE
GNB3
Synaptophysin
TO-PRO
ONL
50 µm
ONL
50 µm
NASAL
OPTIC NERVE
TEMPORAL
1 mm
B P23H + HU210
ONL
50 µm
ONL
50 µm
NASAL
TEMPORAL

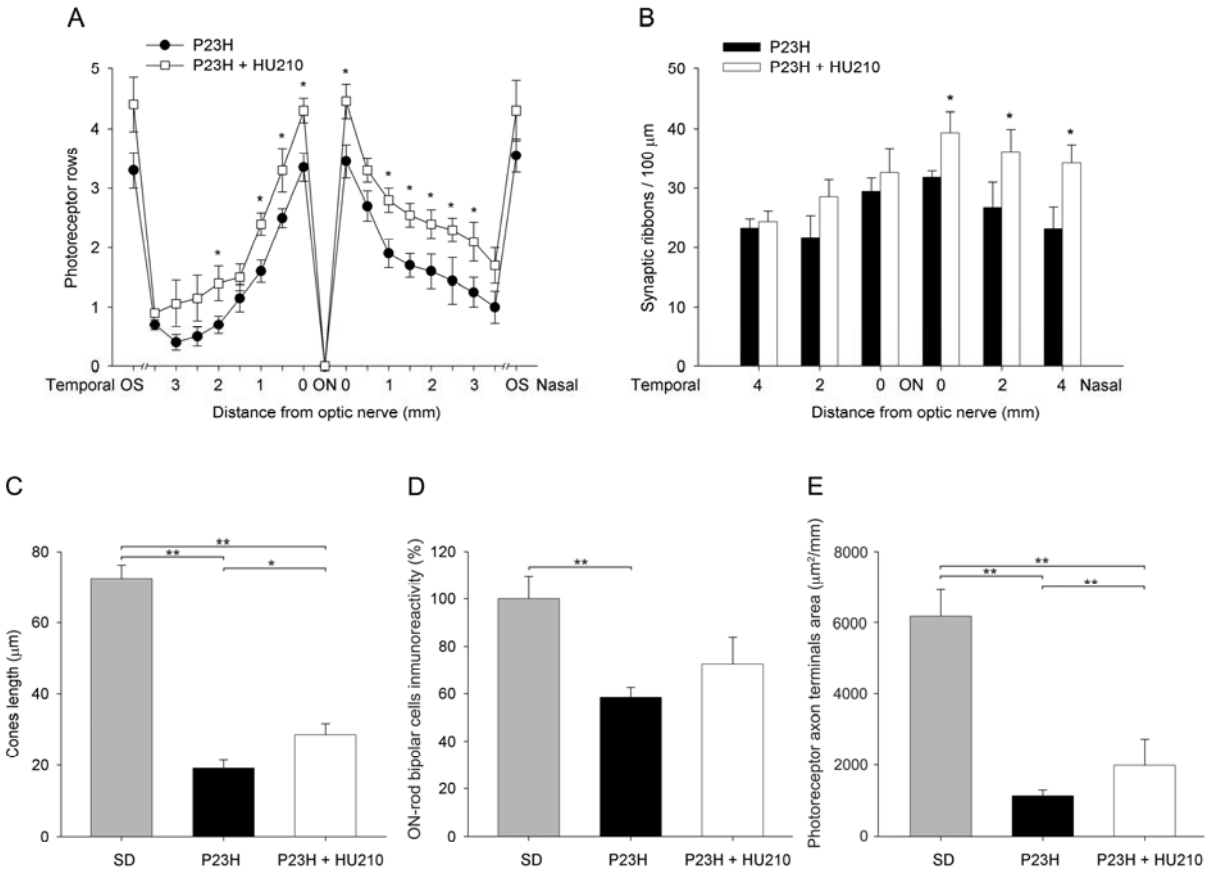
A
P23H
P23H + HU210
Photoreceptor rows
Temporal OS 3 2 1 0 ON 0 1 2 3 OS Nasal
Distance from optic nerve (mm)
B
P23H
P23H + HU210
Synaptic ribbons / 100 µm
Temporal 4 2 0 ON 0 2 4 Nasal
Distance from optic nerve (mm)
C
Cones length (µm)
SD
P23H
P23H + HU210
D
ON-rod bipolar cells immunoreactivity (%)
SD
P23H
P23H + HU210
E
Photoreceptor axon terminals area (µm²/mm)
SD
P23H
P23H + HU210

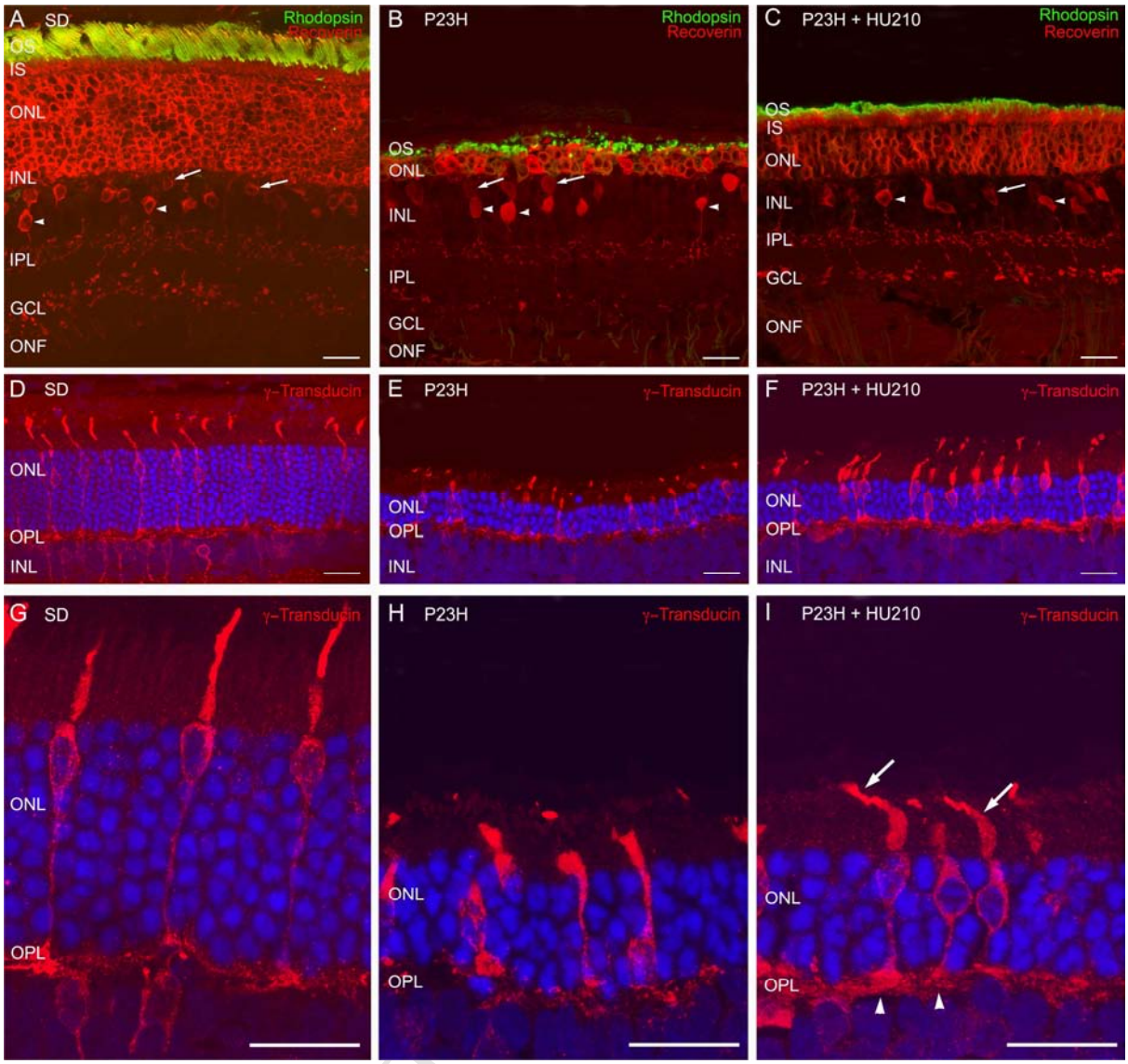
A SD
Rhodopsin
Recoverin
OS
IS
ONL
INL
IPL
GCL
ONF
B P23H
Rhodopsin
Recoverin
OS
ONL
INL
IPL
GCL
ONF
C P23H + HU210
Rhodopsin
Recoverin
OS
IS
ONL
INL
IPL
GCL
ONF
D SD
γ-Transducin
ONL
OPL
INL
E P23H
γ-Transducin
ONL
OPL
INL
F P23H + HU210
γ-Transducin
ONL
OPL
INL
G SD
γ-Transducin
ONL
OPL
H P23H
γ-Transducin
ONL
OPL
I P23H + HU210
γ-Transducin
ONL
OPL

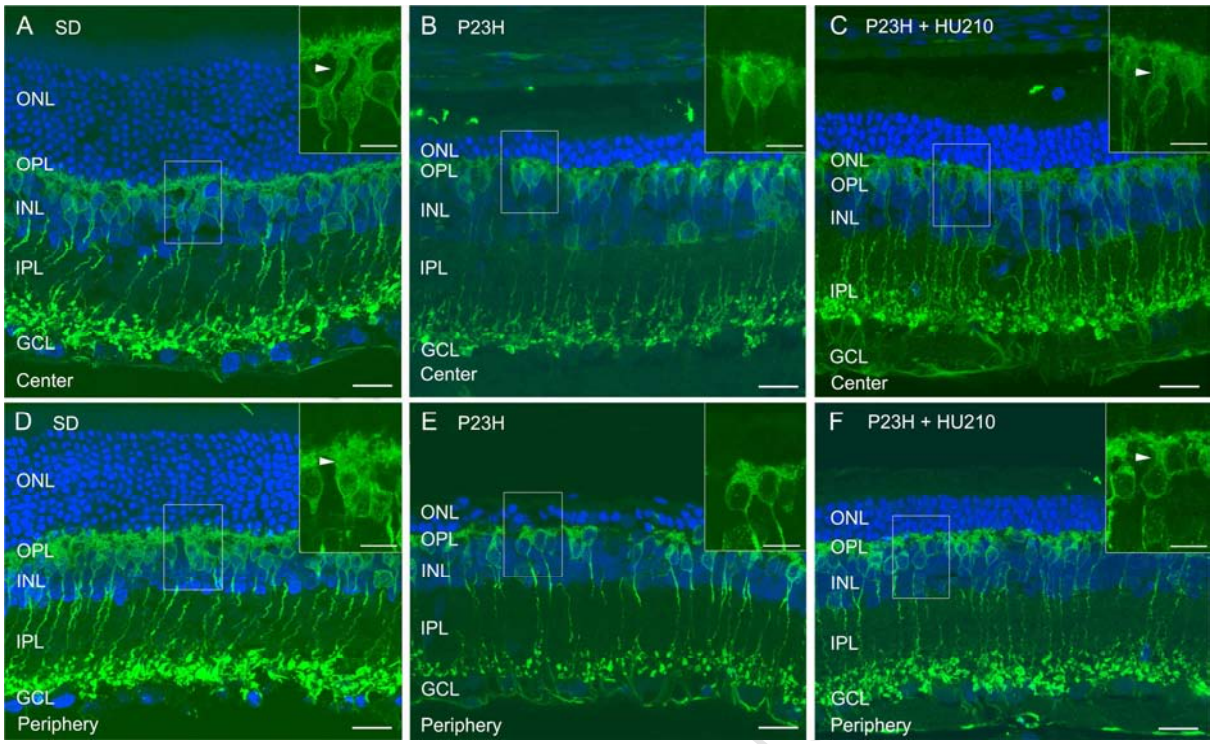

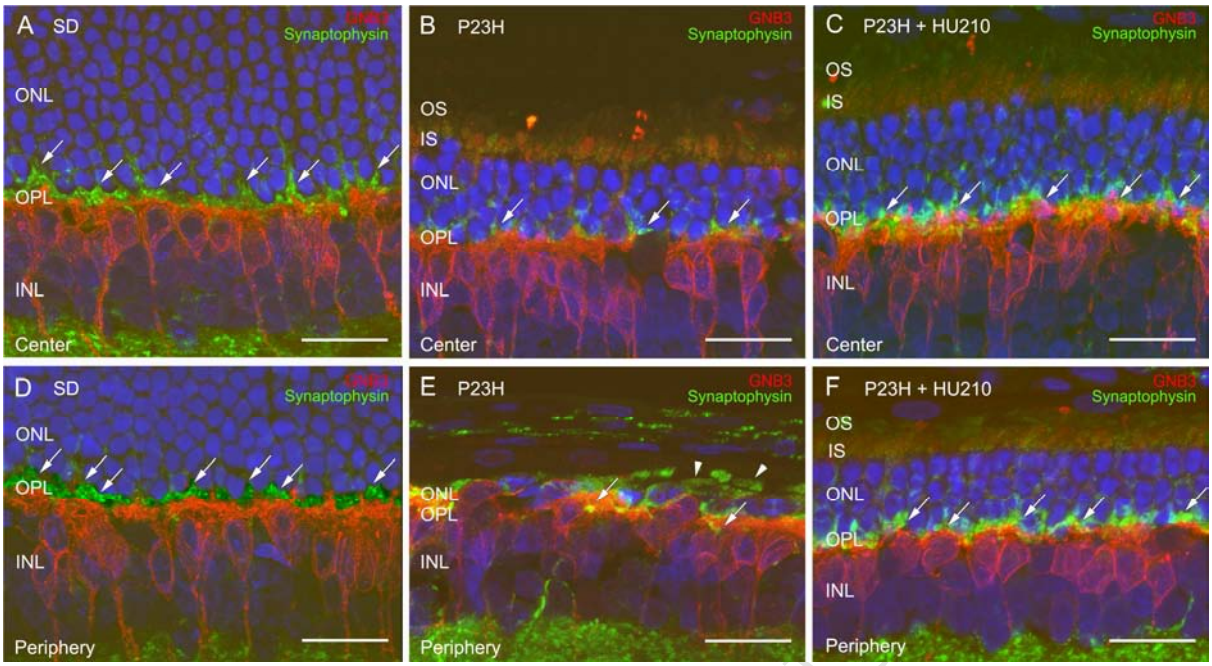

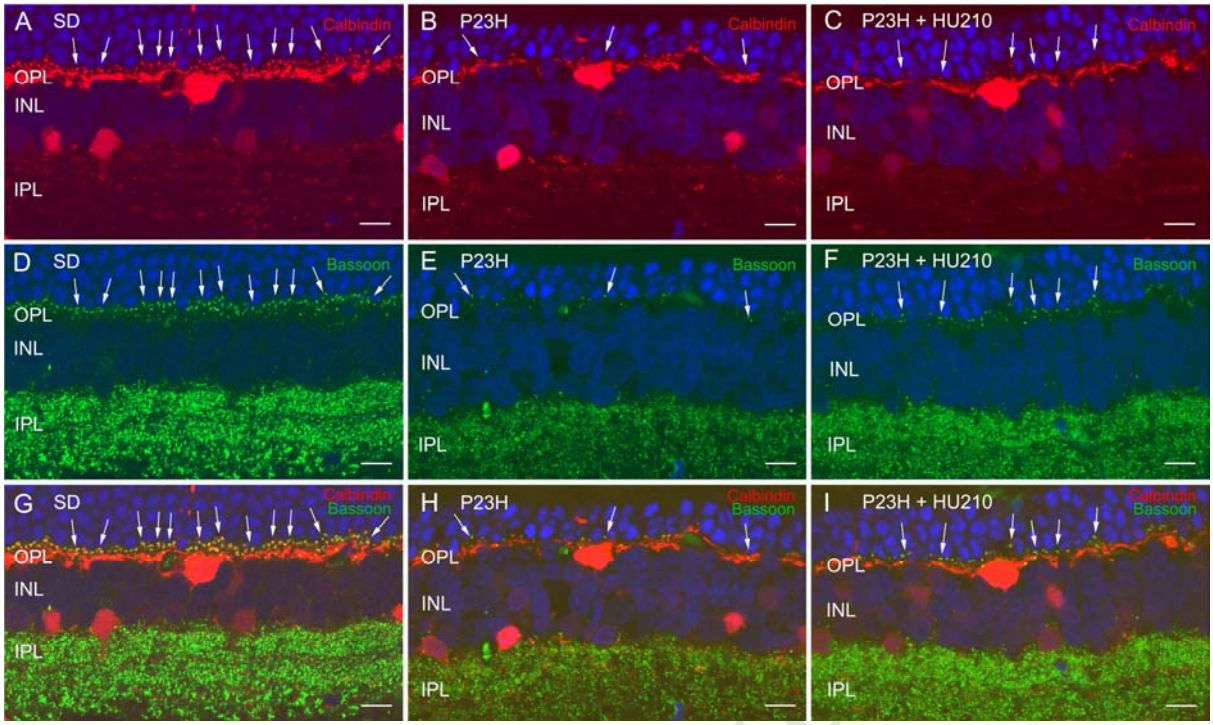

Research highlights:

> HU210 preserves retinal function.

> HU210 preserves cone and rod structure.

> HU210 preserves photoreceptor contacts with postsynaptic neurons.

> Cannabinoids are potentially useful to delay retinal degeneration.